TYPE Opinion
PUBLISHED 07 January 2025
DOI 10.3389/fspas.2024.1532334

OPEN ACCESS

EDITED BY
Andrea Longobardo,
National Institute of Astrophysics (INAF), Italy

REVIEWED BY
Paulina Wolkenberg,
Institute for Space Astrophysics and Planetology (INAF), Italy

*CORRESPONDENCE
Victor Corchete,
corchete@ual.es

RECEIVED 21 November 2024
ACCEPTED 11 December 2024
PUBLISHED 07 January 2025

CITATION
Corchete V (2025) CO_2 polar mass on Mars determined from InSight pressure data. *Front. Astron. Space Sci.* 11:1532334. doi: 10.3389/fspas.2024.1532334

CO_2 polar mass on Mars determined from InSight pressure data

Victor Corchete*

Higher Polytechnic School, University of Almeria, Almería, Spain

KEYWORDS

CO_2 polar mass, InSight mission, Mars, pressure, atmosphere

1 Introduction

The knowledge of the Martian climate is the key to facilitate human exploration and determine whether Mars could be a habitable planet for humans in the future. Analyses of ground-based and satellite observations from the missions developed in more than 50 years have led to a robust knowledge of this climate, which is regulated by the CO_2, dust, and H_2O cycles, coupled to radiative and dynamical processes. On a planetary scale, the Martian atmospheric circulation is strongly affected by the seasonal sublimation and deposition of CO_2 at the polar caps because CO_2 is the principal component of the Martian atmosphere (95.3% CO_2, 2.7% N_2, 1.6% argon (Ar), and 0.4% other gases; Belton et al., 2024); it condenses during the autumn and winter seasons (and precipitates as frosted CO_2) and sublimes during the spring and summer seasons due to solar radiation. The northern seasonal frosted CO_2 dissipates completely during spring and summer seasons, but the South Pole retains a thin permanent cover of frosted CO_2. In this paper, the total mass involved in the cycle of CO_2 (exchanged between the Martian atmosphere and surface) is determined from the pressure data, provided by the Interior Exploration using Seismic Investigations, Geodesy and Heat Transport (InSight) mission. This mass is compared with that determined by Kelly et al. (2006) from gamma ray and neutron data (measured by components of the gamma ray spectrometer instrument suite on 2001 Mars Odyssey) and that predicted by the general circulation models (GCMs): the NASA Ames Research Center (NARC) and Mars Climate Database V6.1 (MCD).

2 Data, methodology, and results

The pressure data used in this study have been extracted from the pressure sensor of InSight. This sensor is designed to produce a valid output between pressures of approximately 560 Pa and 1,000 Pa, which are expected to be the extreme pressures that are experienced at the InSight landing site. The sensor is specifically designed to minimize noise, with a typical root mean square (RMS) of approximately 10 mPa on any particular reading (Banfield et al., 2019). However, according to the recent study performed by Lange et al. (2022) about the recalibration of InSight pressure data, the root mean square (RMS) is found to be approximately 1.5 Pa. They provided the correction on this dataset, which has been considered in the pressure data used in this study. Supplementary Figure S1 shows the pressure data corresponding to the sols 500–510 (sol is a Martian day, i.e., 88,775.244 s or 24.66 h; Hansen et al., 2024). From all pressure data available from InSight, the daily maximum and minimum values are picked (Supplementary Figure S1) to build the curves shown in Supplementary Figure S2A, i.e., the curves of daily maximum and minimum pressures. These curves given *versus* time in sol are converted to curves with

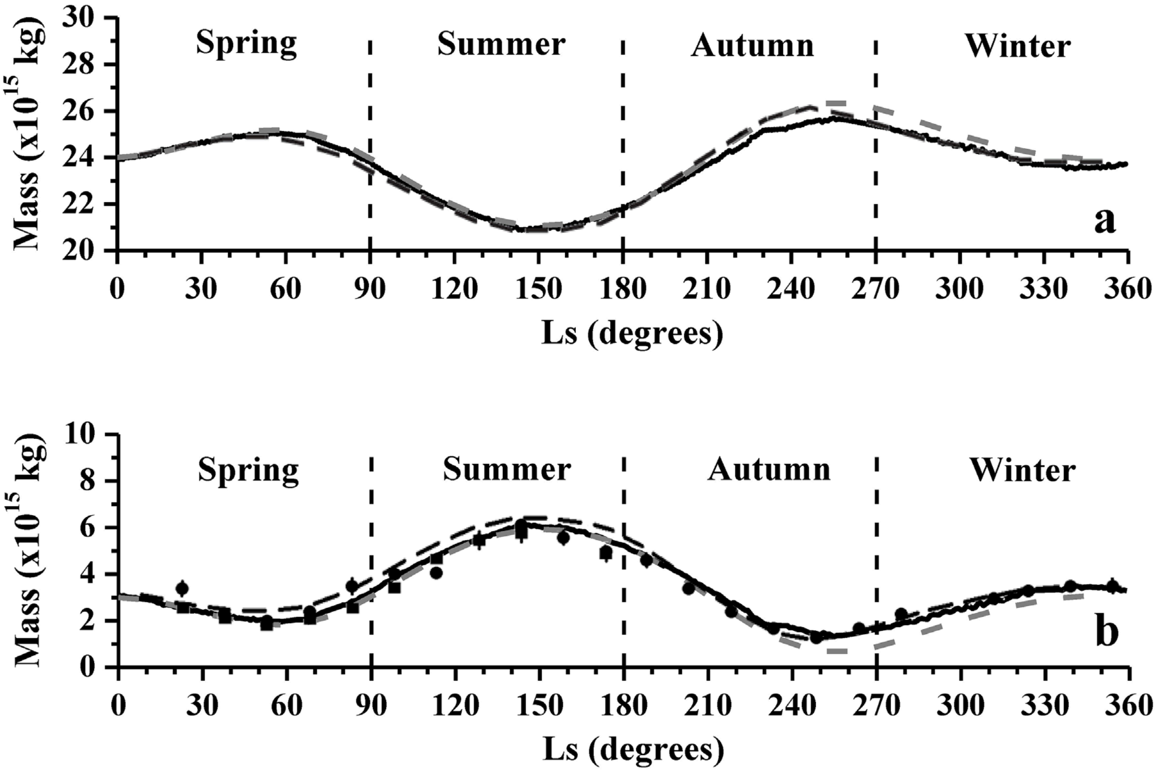

FIGURE 1
Total mass (M_{atm}) of the atmosphere (a, black dot line) and total mass (M_{frost}) of the frosted CO_2 in the polar caps (b, black dot line), determined by Equation 1 from the mean atmospheric pressure (p_{atm}) curve (Supplementary Figure S2B, green dots). The values of M_{frost} calculated by Kelly et al. (2006) are plotted in Figure 1B in black circles and rectangles (vertical bars denote the errors). The values of M_{atm} and M_{frost} predicted by the GCMs are also plotted for comparison (dashed lines): the NARC (black) and MCD (gray). The solar longitude is denoted by Ls, and the northern seasons are also indicated.

time given in the solar longitude (Supplementary Figure S2B; the solar longitude of Mars in its orbit, Ls, Martínez et al., 2017; Hansen et al., 2024), and then, the curve of mean pressure (Supplementary Figure S2B, green dots) is determined from the mean of the abovementioned curves of maximum and minimum pressures. This curve is also interpolated to fill small gaps present in data. This curve can be considered the daily mean atmospheric pressure at the InSight landing site, and it follows an annual repeatable cycle, as observed in previous other datasets (e.g., the Viking and Curiosity datasets; Martínez et al., 2017). This cycle shows two pressure dips (Supplementary Figure S2B): the first dip is the minimum of this cycle reached during southern winter (northern summer), and the second dip is a more minor dip reached during northern winter. The minimum of the cycle is reached during southern winter because it is longer and colder than northern winter, i.e., the deepest minimum of this pressure cycle is associated with the more extensive coverage by seasonal frosted CO_2 in the South Pole (Martínez et al., 2017; Hansen et al., 2024). Supplementary Figure S2B shows that variations in the bulk atmospheric mass due to the condensation and sublimation of CO_2 in the seasonal polar caps cause the observed large pressure variations. This total atmospheric mass (M_{atm}) can be calculated by scaling the mean atmospheric pressure (p_{atm}) curve (Supplementary Figure S2B, green dots) using the formula

$$M_{atm} = m_0 + a(p_{atm} - p_0), \quad (1)$$

where a is a constant and (m_0, p_0) are the mean values of the atmospheric mass and pressure in a Martian year (0°–360° of Ls), respectively. The total mass (M_{frost}) of frosted CO_2 in the polar caps can be determined from M_{atm}, assuming that $M_{atm} + M_{frost} = 27 \times 10^{15}$ kg (Kelly et al., 2006). The value of p_0 is determined from the pressure data shown in Supplementary Figure S2B (green dots) as 717.73 Pa. The values of a and m_0 are calculated numerically by Equation 1 as the values that yield the best fit of the total mass of frosted CO_2 in the polar caps calculated by Kelly et al. (2006). These values are $a = 0.03 \times 10^{15}$ kg/Pa and $m_0 = 23.5 \times 10^{15}$ kg. Figure 1 shows the values of M_{atm} and M_{frost} determined in the present study as a function of Ls, as well as the values of M_{frost} calculated by Kelly et al. (2006). The values of M_{atm} and M_{frost} predicted by the GCMs are also shown in Figure 1, for comparison.

3 Discussion and conclusion

Figure 1B shows the good fit existing between the values determined in this study for M_{frost} and those calculated by Kelly et al. (2006). It shows that the pressure data (e.g., provided by InSight) can be used as a valid method to determine the total mass exchanged between the Martian atmosphere and surface (i.e., the total mass involved in the cycle of CO_2). Furthermore, a good fit is shown in Figure 1B between the M_{frost} value calculated here and that predicted by the GCMs. However, it is observed that the NARC model slightly overestimates the M_{frost} values from 40° to 190° Ls, and the MCD model clearly underestimates M_{frost} from 240° to 340° Ls. This misfit of the GCMs may be due to the dust storms occurring on Mars because they have important effects on the meteorology and climatology of Mars. It is observed that the error bars in Figure 1B are, in general, very small (for some measures, the error is smaller than the symbol used to plot this measure), i.e., the uncertainties in Figure 1B show that the misfit is due to the dust (which is not represented correctly in GCMs), and it is not simply an uncertainty of results. Dust, once lifted into the atmosphere, remains suspended for a long period, absorbing and scattering solar radiation, thereby heating the atmosphere (Martín-Rubio et al., 2024). This feature of dust storms affects the sublimation and condensation processes of CO_2 in the polar regions (He et al., 2024). Unfortunately, the mechanisms of the large storm growth and development already remain poorly understood (Wang et al., 2023). A better understanding of dust storms is needed to understand the Martian meteorology and climatology (Guha et al., 2024). Modeling efforts have been performed in recent decades, incorporating these effects into GCMs, such as the NARC and MCD models. However, more work is already needed to model the dust storms precisely with a GCM. Probably, this task could be feasible when more data will be available provided by future missions.

Author contributions

VC: conceptualization, data curation, formal analysis, funding acquisition, investigation, methodology, project administration, resources, software, supervision, validation, visualization, writing–original draft, and writing–review and editing.

Funding

The author(s) declare that no financial support was received for the research, authorship, and/or publication of this article.

Acknowledgments

The InSight mission has provided the data used in this study, which are available from the Planetary Data System (PDS) of the National Aeronautics and Space Administration (NASA) at https://pds-geosciences.wustl.edu/missions/insight/index.htm.

Conflict of interest

The author declares that the research was conducted in the absence of any commercial or financial relationships that could be construed as a potential conflict of interest.

Generative AI statement

The author(s) declare that no Generative AI was used in the creation of this manuscript.

Publisher's note

Supplementary material

The Supplementary Material for this article can be found online at: https://www.frontiersin.org/articles/10.3389/fspas.2024.1532334/full#supplementary-material

References

Banfield, D. (2019). *InSight APSS PS data product bundle*. Cornell University: NASA Planetary Data System. doi:10.17189/1518939

Belton, M. J. S., Carr, M. H., and Malin, M. C. (2024). Mars. *Encycl. Br.* Available at: https://www.britannica.com/place/Mars-planet.

Guha, B. K., Gebhardt, C., Young, R. M. B., Wolff, M. J., and Montabone, L. (2024). Seasonal and diurnal variations of dust storms in Martian year 36 based on the EMM-EXI database. *J. Geophys. Res. Planets* 129, e2023JE008156. doi:10.1029/2023je008156

Hansen, C. J., Byrne, S., Calvin, W. M., Diniega, S., Dundas, C. M., Hayne, P. O., et al. (2024). A comparison of CO2 seasonal activity in Mars' northern and southern hemispheres. *Icarus* 419, 115801. doi:10.1016/j.icarus.2023.115801

He, F., Rong, Z., Wu, Z., Gao, J., Fan, K., Zhou, X., et al. (2024). Martian dust storms: reviews and perspective for the tianwen-3 Mars sample return mission. *Remote Sens.* 16, 2613. doi:10.3390/rs16142613

Kelly, N. J., Boynton, W. V., Kerry, K., Hamara, D., Janes, D., Reedy, R. C., et al. (2006). Seasonal polar carbon dioxide frost on Mars: CO2 mass and columnar thickness distribution. *J. Geophys. Res.* 111, E03S07. doi:10.1029/2006je002678

Lange, L., Forget, F., Banfield, D., Wolff, M., Spiga, A., Millour, E., et al. (2022). Insight pressure data recalibration, and its application to the study of long-term pressure changes on Mars. *J. Geophys. Res. Planets* 127, e2022JE007190. doi:10.1029/2022je007190

Martínez, G. M., Newman, C. N., De Vicente-Retortillo, A., Fischer, E., Renno, N. O., Richardson, M. I., et al. (2017). The modern near-surface martian climate: a review of in-situ meteorological data from viking to curiosity. *Space Sci. Rev.* 212, 295–338. doi:10.1007/s11214-017-0360-x

Martín-Rubio, C., Vicente-Retortillo, A., Gómez, F., and Rodríguez-Manfredi, J. A. (2024). Interannual variability of regional dust storms between Mars years 24 and 36. *Icarus* 412, 115982. doi:10.1016/j.icarus.2024.115982

Wang, H., Saidel, M., Richardson, M. I., Toigo, A. D., and Michael, B. J. (2023). Martian dust storm distribution and annual cycle from Mars daily global map observations. *Icarus* 394, 115416. doi:10.1016/j.icarus.2022.115416